



A LETTERS JOURNAL EXPLORING  
THE FRONTIERS OF PHYSICS

OFFPRINT

**Basin boundary metamorphoses and phase  
control**

J. M. SEOANE, S. ZAMBRANO, I. P. MARIÑO and M. A. F. SANJUÁN

EPL, **90** (2010) 30002

Please visit the new website  
[www.epljournal.org](http://www.epljournal.org)

# TARGET YOUR RESEARCH WITH EPL



Sign up to receive the free EPL table of  
contents alert.

[www.epljournal.org/alerts](http://www.epljournal.org/alerts)

# Basin boundary metamorphoses and phase control

J. M. SEOANE, S. ZAMBRANO, I. P. MARIÑO and M. A. F. SANJUÁN

*Departamento de Física, Universidad Rey Juan Carlos - Tulipán s/n, 28933 Madrid, Spain, EU*

received 23 March 2010; accepted 20 April 2010

published online 25 May 2010

PACS 05.45.-a – Nonlinear dynamics and chaos

PACS 05.45.Df – Fractals

PACS 05.45.Pq – Numerical simulations of chaotic systems

**Abstract** – Basin boundary metamorphoses are characteristic in some kinds of chaotic dynamical systems. They take place when one parameter of the system is varied and it passes through a certain critical value. In this paper we show that a parametric harmonic perturbation can produce basin boundary metamorphoses in periodically driven chaotic dynamical systems even when its amplitude is smaller than the amplitude of the main driving. The physical context of this work is related with the phenomenon of trajectories escaping from a potential well, which is illustrated by using as prototype model the Helmholtz oscillator. One of the main contributions of our research is to analyze the role of the phase difference between the parametric harmonic perturbation and the main driving in the appearance of a basin boundary metamorphosis. We also analyze the variation of the size of the basins and the fractal dimension of the corresponding boundaries when this phenomenon occurs. Finally, Melnikov analysis of this phenomenon is carried out. We expect that this work can be useful for a better understanding of basin boundary metamorphoses phenomena.

Copyright © EPLA, 2010

**Introduction.** – In the past years several works have been carried out on the mechanisms for which attractors arise and their basins change insofar as one specific parameter of the system is varied. One of these mechanisms, for which basin boundaries can go from a fractal to a non-fractal structure (or vice versa) once a parameter crosses a certain critical value, is called *basin boundary metamorphosis* (BBM) [1,2]. In this sense some works have analyzed how fractal basin boundaries arise and change as a parameter of the system is varied, as for example in the case of the forced damped pendulum [1]. One of the main consequences of the BBM is the drastic change in the size of the basin boundary. On the other hand, the BBM phenomenon is also related with the phenomenon of explosions of chaotic sets [3]. In this paper, we study in detail the BBM produced by a parametric harmonic perturbation of an open dynamical system. In an open dynamical system, there is a region in phase space where nearly all the trajectories diverge asymptotically to infinity. They have attracted a great deal of attention in the context of transient chaos [4] and, particularly, in chaotic scattering problems [5–8], among others.

In our case, we investigate a problem that arises in the context of the phase control [9–15] of trajectories escaping from a potential well [16]. The main idea of

the phase control method is to apply a small harmonic perturbation in periodically driven nonlinear oscillators, either parametrically or as an external perturbation. This harmonic perturbation has an amplitude  $\varepsilon$  and a phase difference  $\phi$ . We consider the amplitude to be always less than the amplitude of the driving force and the phase  $\phi$  corresponds to the phase difference (*phase*) with respect to the main driving. This phase  $\phi$  plays a crucial role in the dynamical behavior of our system, as shown in ref. [16]. This technique has been used to avoid escapes in open dynamical systems, in which the authors suggested that a phenomenon related to this control was a BBM. Here, our main goal is to investigate this BBM, produced by a small harmonic perturbation.

Despite a large body of existing literature on the study of BBM, a thorough study of the fractal dimension and the size of the basin boundaries has received relatively little attention [1,2,17,18] and it is one of the objectives of this work. In ref. [18], the authors analyze both the area and the fractal dimension of the basins in the context of driven oscillators and their relevance to safe engineering design.

In this paper we make a study in depth of this phenomenon by considering the variation of both, the size of the basins and the fractal dimension of the corresponding boundaries due to the effect of adding a parametric

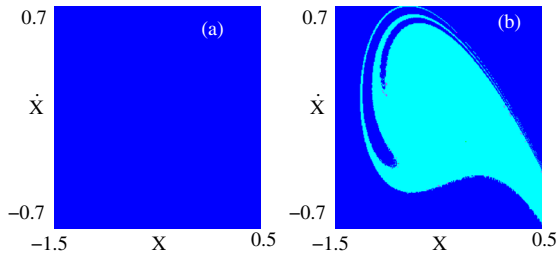


Fig. 1: (Color online) (a) Basin of attraction of the Helmholtz oscillator,  $\ddot{x} + 0.1\dot{x} - x - x^2 = 0.21 \cos t$ . We denote by blue (black) dots the set of points that escape from this region of phase space, including points inside the potential well, to infinity, and cyan (pale gray) dots as the points that fall into the attractor(s). Note that in this picture all initial conditions escape after some period of time. (b) Basin of attraction of the Helmholtz oscillator,  $\ddot{x} + 0.1\dot{x} - x - x^2 = 0.12 \cos t$ . Here the basins in phase space have a fractal structure where cyan points (pale gray) denote the set of points falling into the attractors.

harmonic perturbation. A Melnikov analysis is carried out in order to explain the role of the phase  $\phi$  since it is crucial to produce the BBM.

**Model description.** – A simple paradigmatic example of a dynamical system with escapes is the Helmholtz oscillator. It describes the motion of a unit mass particle in a cubic potential  $V(x) = ax^2/2 + bx^3/3$  [19], which eventually can be externally perturbed by a sinusoidal driving. By adding a linear dissipative force, the equation of motion for a suitable choice of the parameters is [16]

$$\ddot{x} + 0.1\dot{x} - x - x^2 = F \cos t. \quad (1)$$

This system presents different behaviors depending on the value of the forcing amplitude  $F$ . For example, a plot of the basins of attraction for  $F = 0.21$  is depicted in fig. 1(a) and for  $F = 0.12$  in fig. 1(b), where blue (black) color represents the set of points that escape from this region of phase space, including points inside the potential well, to infinity and cyan (pale gray) color represents the set of points that fall into the attractors. In general, a trajectory escapes from this region of phase space when it diverges to infinity.

For the forcing amplitude  $F = 0.21$  it is possible to avoid escapes in a certain region of the phase space according to the strategy described in ref. [16], that was there implemented in an electronic circuit.

This means that if we add a parametric perturbation in the quadratic term of the equation of motion we have

$$\ddot{x} + 0.1\dot{x} - x - (1 + \varepsilon \cos(t + \phi))x^2 = F \cos(\omega t), \quad (2)$$

where  $\varepsilon$  is the modulation amplitude and  $\phi$  (phase) is the phase difference with respect to the main forcing.

Figure 2(a) shows a single trajectory for the Helmholtz oscillator when  $F = 0.21$  and no control is applied. We can see how the trajectory escapes after a certain lapse of time. Figure 2(b) shows the trajectory for the same

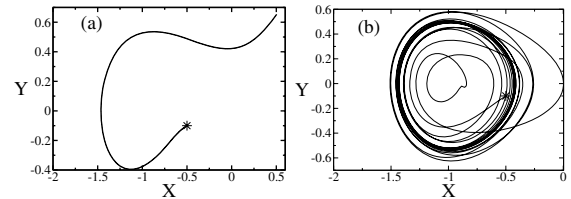


Fig. 2: (a) Single trajectory for the Helmholtz oscillator,  $\ddot{x} + 0.1\dot{x} - x - x^2 = 0.21 \cos t$ , with initial condition at the point  $(x_0, \dot{x}_0) = (-0.5, -0.1)$  as indicated by the star. The trajectory escapes after a lapse of time. (b) The same initial condition for the Helmholtz oscillator with control,  $\ddot{x} + 0.1\dot{x} - x - (1 + 0.05 \cos(t + \pi))x^2 = 0.21 \cos t$ . The perturbation keeps the particle in the well forever.

initial condition when the phase control method is applied. In particular, we are considering  $\phi = \pi$  (this is the most suitable value of the phase to prevent the majority of the escapes from the single well [16]) and we can see how for a certain value of  $\varepsilon$  the particle stays inside the well forever.

**Effects of the parametric perturbation on the escaping dynamics.** – In this section we provide numerical evidence showing that, by using an adequate value of  $\phi$  and  $\varepsilon$ , we can avoid escapes for the Helmholtz system, and we relate it with a BBM phenomenon.

We have performed a numerical integration of trajectories whose initial conditions belong to a  $60 \times 60$  grid in the phase space region  $x \in [-1.5, 0]$ ,  $\dot{x} \in [-0.7, 0.7]$  for different sets of parameter values of  $\varepsilon$  and  $\phi$ , and observe which of them escape. The diagrams plotted in figs. 3(a)–(c) show the rate of trajectories that escape from the well as a function of  $\varepsilon$  and  $\phi$ . Note that in some regions of these diagrams, *e.g.*, for  $\varepsilon \approx 0.12$  and  $\phi = \pi$  more than 60% of the initial conditions are kept bounded inside the well. However, if we take another value of the phase, such as  $\phi = 0$ , nearly all trajectories escape. Thus, the role of the phase  $\phi$  is crucial if we want to keep the trajectories inside the well.

In order to have a deeper insight of this phenomenon we have estimated the escape times of the trajectories for different initial conditions fixing the phase  $\phi$  and the modulation amplitude  $\varepsilon$ , separately. For our numerical simulations, we consider the escape time  $T$  as the time that a certain initial condition in phase space spends before crossing a far away point from the potential well, that we have taken as  $x = 1$ . Notice that a certain rate of the trajectories never escapes, having infinite escape times. Since it is not possible to numerically compute most of the escape times, the integration times have been bounded. In particular, we have taken the integration time equal to  $t_{max} = 6 \times 10^4$  time units as a reasonable bound to assure the trajectories to be kept inside the well forever. We have plotted in figs. 4(a)–(d) the behavior of the average escape times  $T$  for 100 different initial conditions chosen in the region  $x \in [-1.5, 0]$  and for  $\dot{x} = 0$ . In fig. 4(a)

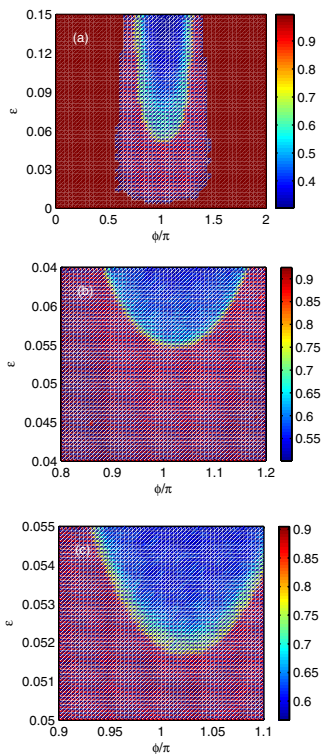


Fig. 3: (Color online) Color plots of the fraction of trajectories with initial conditions in the region of phase space  $[-1.5, 0] \times [-0.7, 0.7]$  that escape to infinity for different values of  $\varepsilon$  and  $\phi$ . (b),(c) show zooms of (a) in which we clearly observe the drastic transition for the trajectories to escape from the well. Taking  $\phi = \pi$ , this takes place at  $\varepsilon \simeq 0.05$ .

we fixed the phase to  $\phi = \pi$  increasing the value of  $\varepsilon$  from 0 to 0.1. We can observe some fluctuations in the escape times for small values of  $\varepsilon$ . This fact is due to the effects of the appearance and disappearance of different attractors in the system as we show in next section. Once the modulation amplitude  $\varepsilon$  reaches the critical value  $\varepsilon_c \simeq 0.05$  (see fig. 4(b) for a zoom of this region)  $T$  has a steep increase limited by the integration time  $t_{max}$ . In this picture we have distinguished two different regions, region I ( $\varepsilon < \varepsilon_c$ ) and region II ( $\varepsilon > \varepsilon_c$ ). This result is in agreement with the BBM phenomenon that we will describe in next section in more detail. For  $\varepsilon < \varepsilon_c$ , only a fraction of the initial conditions yields confined trajectories and the complementary fraction escape at times less than  $t_{max}$ . Thus,  $T$  results as a weighted sum, where the confined fraction enters with the value  $t_{max}$ . The observation of fig. 4(a) in the region of  $\varepsilon > \varepsilon_c$  suggest that almost all trajectories get confined inside the well. For  $\varepsilon < \varepsilon_c$ , the irregular  $T$  vs.  $\varepsilon$  profile is due to the fractal structure of the basins, as shown in fig. 5(a). Figures 4(c), (d) show, for  $\varepsilon = 0.043 < \varepsilon_c$  and for  $\varepsilon = 0.057 > \varepsilon_c$  the crucial role of the phase  $\phi$  in the escape times showing that the optimal value takes place at  $\phi_{opt} \approx \pi$ , where the confined trajectories are clustered around this value. Notice that this is not so clearly observed in fig. 4(c) due to the presence of the

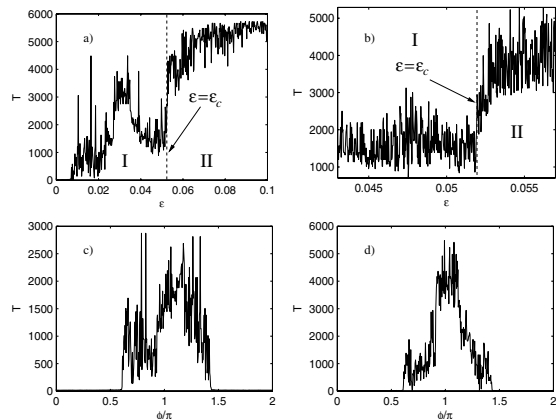


Fig. 4: (a) Plot of the average escape times  $T$  vs. the modulation amplitude  $\varepsilon$  for a fixed value of the phase  $\phi = \pi$  and 100 different initial conditions chosen in the region  $x \in [-1.5, 0]$  and  $\dot{x} = 0$ . In this figure we can observe some fluctuations of the average escape times for low values of  $\varepsilon$  and a rapid increasing to infinity (the integration time) for the escape times once that  $\varepsilon$  is large enough (above its critical value  $\varepsilon_c \simeq 0.05$ ). (b) This figure represents a zoom of (a). (c) Plot of the average escape times  $T$  vs. the phase  $\phi$  for a fixed value of the modulation amplitude  $\varepsilon = 0.043$  and 100 different initial conditions chosen in the region  $x \in [-1.5, 0]$  and  $\dot{x} = 0$ . (d) Plot of the average escape times  $T$  vs. the phase  $\phi$  for a fixed value of the modulation amplitude  $\varepsilon = 0.057$  and 100 different initial conditions chosen in the region  $x \in [-1.5, 0]$  and  $\dot{x} = 0$ .

fluctuations of the average escape times that occurs in region I (see fig. 4(a)). In the next section we show that this phenomenon is related to a BBM.

**Fractal dimension and size of the basins.** – The metamorphosis implies a drastic change in the size of the basin boundaries and also in the fractal dimension [1,17,18] due to the basin transition from a fractal to a non-fractal structure or vice versa. Here, we study how these changes take place in our model once we vary the parameter  $\varepsilon$ . For this purpose, we plot the basins of attraction of our system for different parameter values  $\varepsilon$  and we analyze the different dynamical behaviors.

The basins of attraction of the controlled Helmholtz oscillator,  $\ddot{x} + 0.1\dot{x} - x - (1 + \varepsilon \cos(t + \pi))x^2 = 0.21 \cos t$ , for values of  $\varepsilon = 0.045$  and  $\varepsilon = 0.0497$  (region I), and  $\varepsilon = 0.09$  and  $\varepsilon = 0.13$  (region II), are plotted in figs. 5(a)–(d), respectively. We observe multiple attractors in fig. 5(b) (for values of  $\varepsilon$  in region I) which are denoted by using different colors. This explains the fluctuations in the escape times shown in figs. 4(a), (b). Insofar we increase  $\varepsilon$ , the only observable attractor is the fixed point at the bottom of the potential well which has a strong effect because most of trajectories remain inside the well forever. On the other hand, figs. 6(b),(c) show a drastic change in the size of the basins of attraction once  $\varepsilon$  crosses a certain critical value  $\varepsilon_c$ . We can also observe qualitatively a loss of the fractality in the boundaries

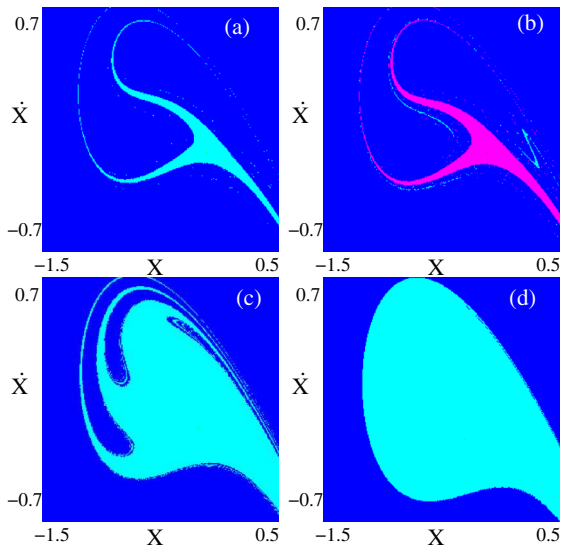


Fig. 5: (Color online) Basins of attraction of the controlled Helmholtz oscillator,  $\ddot{x} + 0.1\dot{x} - x - (1 + \varepsilon \cos(t + \pi))x^2 = 0.21 \cos t$ , with modulation amplitudes located at region I,  $\varepsilon = 0.045$  (a) and  $\varepsilon = 0.0497$  (b) and at region II,  $\varepsilon = 0.09$  (c) and  $\varepsilon = 0.13$  (d), respectively. Blue (black) dots denote the initial conditions that escape from the potential well and cyan (pale gray) dots the ones that fall into the attractor(s). We observe multiple attractors in (b) which are denoted by using different colors.

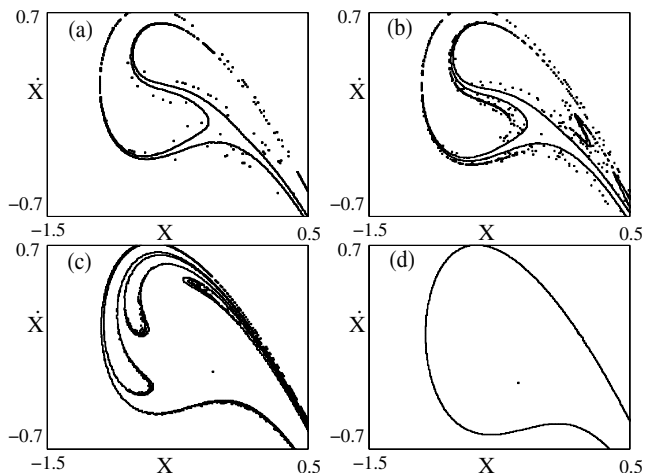


Fig. 6: Boundaries of the basins of attraction shown in fig. 5 with modulation amplitudes located at region I,  $\varepsilon = 0.045$  (a),  $\varepsilon = 0.0497$  (b) and at region II,  $\varepsilon = 0.09$  (c) and  $\varepsilon = 0.13$  (d), respectively.

when  $\varepsilon > \varepsilon_c$ , which is clearly observed in fig. 6(c) and fig. 6(d). The onset of this phenomenon takes place for values of  $\varepsilon_c \simeq 0.05$ , which is in complete agreement with the numerical evidence provided in the previous section, in which most of trajectories are trapped (see fig. 3).

Figures 6(a)–(d) show the boundaries of the corresponding basins of attraction plotted in figs. 5(a)–(d), respectively. We have computed the fractal dimension (box-counting dimension [20]) of the boundaries for

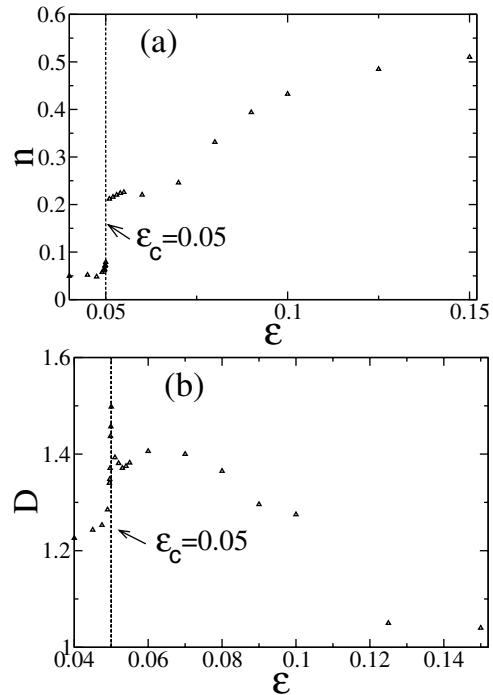


Fig. 7: (a) Size of the basins of attraction *vs.* the modulation amplitude  $\varepsilon$  as in fig. 5. (b) Variation of the fractal dimension of the basin boundaries (see fig. 6) *vs.*  $\varepsilon$ .

different values of  $\varepsilon$ ,  $D(\varepsilon)$ , obtaining:  $D(0.045) = 1.243$ ,  $D(0.0497) = 1.371$ ,  $D(0.09) = 1.296$  and  $D(0.13) = 1.05$ , respectively. Notice that in spite of the apparent smoothness of the boundary, as seen in fig. 5(d), this boundary is slightly fractal, as shown in these computations. As we expected, we also observe a decreasing in the fractal dimension once the onset of BBM occurs.

The drastic change in the basins is shown in figs. 5(b),(c) where a rapid increase of the size of the basin of attraction is easily observed. The physical meaning of this increase is also due to the strong effect of the attractors once  $\varepsilon > \varepsilon_c$ , for which most of trajectories are trapped into the well and never escape. To estimate the variation of the size of the basins of attraction we compute  $n = N_0/N_t$ , where  $N_0$  denotes the number of initial conditions trapped into the well and  $N_t$  is the total number of initial conditions. The computation of the value of  $n$  is a good way to estimate the relative variation of the size of the basin of attraction.

Figures 5(a)–(d) show in a qualitative manner the variation of the size of the basin of attraction for different values of  $\varepsilon$ ,  $n(\varepsilon)$ , that is:  $n(0.045) = 0.051$ ,  $n(0.0497) = 0.052$ ,  $n(0.09) = 0.41$  and  $n(0.13) = 0.47$ , respectively. We observe a rapid increasing in the size of the basin of attraction when  $\varepsilon$  becomes larger.

The variation of both, the size and the fractal dimension of the boundaries, against the parameter  $\varepsilon$  are plotted in figs. 7(a),(b), respectively. We observe a rapid increase in the size of the basins and a rapid decrease in the fractal dimension due to the effect of the metamorphosis, which takes place at  $\varepsilon_c \simeq 0.05$ . A similar behavior for the fractal

dimension by using both a one-dimensional map and a continuous-time system in the absence of the parametric perturbation were found in refs. [17,18], respectively. The increasing in the basin size implies that, since the trajectories are trapped into the well when  $\varepsilon$  increases, the system loses the unpredictability (due to most trajectories never escape) and therefore the boundaries become non-fractal. For this reason, we expect that once  $\varepsilon \geq \varepsilon_c \simeq 0.05$  the fractal dimension decreases. This phenomenon is illustrated in fig. 7(b). This loss of unpredictability produces an increasing in the size of the basin of attraction due to the fact that most initial conditions are trapped into the well and they never escape from it, which is illustrated in fig. 7(a). We conjecture this result to be valid for a large number of systems since the effect of introducing a parametric perturbation in this kind of systems has, qualitatively, the same physical consequences independently of the chosen system.

**Melnikov analysis: role of the phase.** – In order to complete our study on the phenomena described above, we are going to perform a Melnikov analysis of our system elucidating the role of the phase on the escaping dynamics.

Equation (2) can be rewritten as:

$$\begin{aligned} \dot{x} &= y, \\ \dot{y} &= x + x^2 + (-\delta y + F \cos(\omega t) + \varepsilon \cos(t + \phi))x^2, \end{aligned} \quad (3)$$

with  $\delta = 0.1$  and  $F = 0.21$ . The Melnikov function  $M(t_0)$  is

$$\begin{aligned} M(t_0) &= \int_{-\infty}^{+\infty} y_h(t)(-\delta y_h(t) + F \cos(\omega t) \\ &\quad + \varepsilon \cos(t + \phi))x_h(t)^2, \end{aligned} \quad (4)$$

where  $(x_h(t), y_h(t))$  is the homoclinic loop observed for  $F = \varepsilon = \delta = 0$ , where

$$\begin{aligned} x_h(t) &= -\frac{3}{2} \cosh^{-2} \left[ \frac{t - t_0}{2} \right], \\ y_h(t) &= \frac{3}{2} \frac{\sinh \left[ \frac{t - t_0}{2} \right]}{\cosh^3 \left[ \frac{t - t_0}{2} \right]}. \end{aligned} \quad (5)$$

The value of the Melnikov function, which has been computed by making use of the calculations performed in ref. [21], is

$$\begin{aligned} M(t_0) &= -F \frac{6\pi}{\sinh(\pi)} \sin(t_0) - \varepsilon \frac{3\pi}{5 \sinh(\pi)} \sin(t_0 + \phi) \\ &\quad - \delta \frac{6}{5} \equiv -A_F \sin(t_0) - A_\varepsilon \sin(t_0 + \phi) - A_\delta, \end{aligned} \quad (6)$$

where  $A_F$ ,  $A_\delta$  and  $A_\varepsilon$  are positive constants.

As is well known the zeros of the Melnikov function imply the existence of transverse homoclinic intersections and thus the appearance of horseshoes and chaotic motion. In the absence of parametric perturbation,  $A_\varepsilon = 0$ , and for

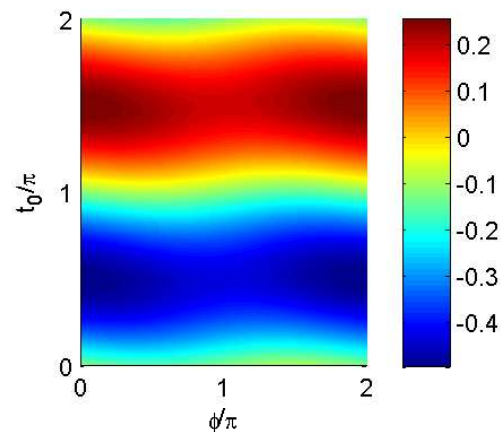


Fig. 8: (Color online) Color plot of the Melnikov distance as a function of  $t_0$  and  $\phi$ , for  $\varepsilon = 0.2$ . For all the  $\phi$  values the function  $M(t_0)$  changes sign for some  $t_0$ , but for  $\phi = \pi$  the absolute values of  $M(t_0)$  above and below zero are smaller than for other values, which suggests that it is the optimal phase value to avoid escapes.

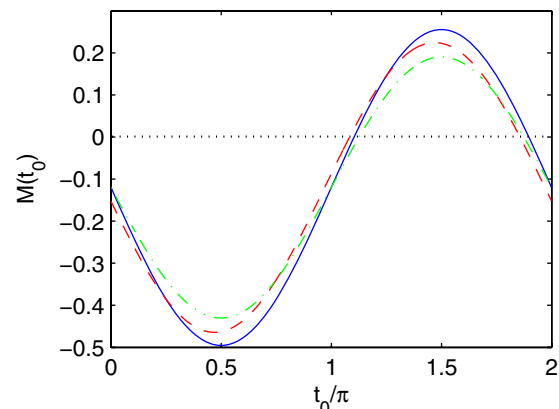


Fig. 9: (Color online) Plot of the Melnikov function  $M(t_0)$  as a function of  $t_0$  for  $\varepsilon = 0.2$  and  $\phi = 0$  (blue, continuous line),  $\phi = \pi/2$  (red, dashed line) and  $\phi = \pi$  (green, dash-dotted line). Clearly the oscillation of  $M(t_0)$  around zero is smaller for the latter, which suggest that this phase is closer to tame the homoclinic intersection and thus it is the optimal phase to avoid escapes, as numerical simulations suggest.

$F = 0.21$  and  $\delta = 0.1$ , we have that  $A_F \approx 0.35 > A_\delta = 0.12$ , so there is a zero in the Melnikov function and a transverse homoclinic intersection.

The condition for the amplitude of the parametric perturbation needed to frustrate the homoclinic intersection is  $A_\varepsilon > |A_F - A_\delta| \approx 0.22$ . However, considering the form of  $A_\varepsilon$  obtained previously, this can be only achieved when  $\varepsilon > 1.37$ . In other words, the range of perturbations that we apply to the system cannot induce the frustration of homoclinic intersections. In our situation, the critical value  $\varepsilon_c \approx 0.05$  for which BBM occurs is characteristic of our specific system and it cannot be predicted analytically. We also point out that, from a physical point of view, this value of  $\varepsilon_c$  is only related with the trajectory trapping in the potential well.

However, we can observe that the best performance for the frustration of the transverse homoclinic intersections with a minimum value of  $\varepsilon$  occurs for the phase value  $\phi = \pi$ . This can be observed in fig. 8, where the Melnikov function is plotted as a function of  $t_0$  and  $\phi$  for  $\varepsilon = 0.2$ . For all the  $\phi$  values the function  $M(t_0)$  changes sign for some  $t_0$ , but for  $\phi = \pi$  the absolute values of  $M(t_0)$  above and below zero are smaller than for other values. In other words, as we can observe in fig. 9, the oscillation of the Melnikov function  $M(t_0)$  around zero is smaller for  $\phi = \pi$  than for other values of  $\phi$ . All this suggests that the influence of the homoclinic intersection in the global dynamics, which is related with the appearance of a horseshoe and eventually with escaping dynamics, is particularly tamed if  $\phi = \pi$ . This also agrees with the fact that it is not possible to observe a significant variation in the basins when a parametric perturbation is applied for other different values of the phase like  $\phi = 0$ .

**Conclusions and discussion.** – In conclusion, we have studied the BBM phenomenon by using as a prototype model the Helmholtz oscillator with an external harmonic perturbation in the quadratic term of the equation of motion. We provide numerical support for which the avoidance of the escapes from the well is directly related to the metamorphosis in the basin boundaries. We have also estimated the fractal dimension of the basin boundaries and the variation in the size of the basin of the attraction finding a drastic change at the point in which the metamorphosis takes place. Theoretical analysis by using Melnikov theory has been carried out and they are in agreement with the numerical results, showing that the value of phase  $\pi$  is the most accurate to produce a change sign in the Melnikov distance. In the context of physical situations, the problems with escapes are typical in chaotic scattering problems, which have applications in many fields in physics. We expect this work to be useful for a better understanding of BBM phenomena.

\*\*\*

We would like to thank J. C. VALLEJO for the fruitful discussions we had during the development of this work. The basins of attraction (fig. 1 and fig. 5) have been made using the software DYNAMICS [22]. This work was supported by the Spanish Ministry of Education and Science under project No. FIS2006-08525 and by the Spanish Ministry of Science and Innovation under project No. FIS2009-09898.

## REFERENCES

- [1] GREBOGI C., OTT E. and YORKE J. A., *Phys. Rev. Lett.*, **56** (1986) 1011.
- [2] GREBOGI C., OTT E. and YORKE J. A., *Physica D*, **24** (1987) 243.
- [3] ROBERT C., ALLIGOOD K. T., OTT E. and YORKE J. A., *Phys. Rev. E*, **64** (2001) 066208.
- [4] TÉL T., in *Directions in Chaos*, edited by HAO BAI-LIN (World Scientific, Singapore) 1990, p. 149.
- [5] JUNG C., *J. Phys.*, **A19** (1986) 1345; HÉNON M., *Physica D*, **33** (1988) 132; GASPARD P. and RICE A., *J. Chem. Phys.*, **90** (1989) 2225; TROLL G. and SMILANSKY U., *Physica*, **35D** (1989) 34.
- [6] DING M., GREBOGI C., OTT E. and YORKE J. A., *Phys. Rev. A*, **42** (1990) 7025.
- [7] OTT E. and TÉL T., *Chaos*, **3** (1993) 417.
- [8] BLEHER S., GREBOGI C. and OTT E., *Physica D*, **46** (1990) 87.
- [9] LIMA R. and PETTINI M., *Phys. Rev. A*, **41** (1990) 726.
- [10] MEUCCI R., GADOMSKI W., CIOFINI M. and ARECCHI F. T., *Phys. Rev. E*, **49** (1994) R2528.
- [11] QU Z., HU G., YANG G. and QIN G., *Phys. Rev. Lett.*, **74** (1995) 1736.
- [12] ZAMBRANO S., ALLARIA E., BRUGIONI S., LEYVA I., MEUCCI R., SANJUÁN M. A. F. and ARECCHI F. T., *Chaos*, **16** (2006) 013111.
- [13] ZAMBRANO S., MARIÑO I. P., SALVADORI F., MEUCCI R., SANJUÁN M. A. F. and ARECCHI F. T., *Phys. Rev. E*, **74** (2006) 016202.
- [14] ZAMBRANO S., SEOANE J. M., MARIÑO I. P., SANJUÁN M. A. F., EUZZOR S., MEUCCI R. and ARECCHI F. T., *New J. Phys.*, **9** (2008) 073030.
- [15] ZAMBRANO S., SEOANE J. M., MARIÑO I. P., SANJUÁN M. A. F. and MEUCCI R., in *Recent Progress in Controlling Chaos*, edited by SANJUÁN M. A. F. and GREBOGI C., Vol. **1** (World Scientific, Singapore) 2010, p. 147.
- [16] SEOANE J. M., ZAMBRANO S., EUZZOR S., MEUCCI R., ARECCHI F. T. and SANJUÁN M. A. F., *Phys. Rev. E*, **78** (2008) 016205.
- [17] PARK B. S., GREBOGI C. and LAI Y. C., *Int. J. Bifurcat. Chaos*, **2** (1992) 533.
- [18] THOMPSON J. M. T. and SOLIMAN M. S., *Proc. R. Soc. London, Ser. A*, **428** (1990) 1.
- [19] ALMENDRAL J. A. and SANJUÁN M. A. F., *J. Phys. A*, **36** (2002) 695.
- [20] OTT E., *Chaos in Dynamical Systems* (Cambridge University Press, Cambridge, UK) 2002.
- [21] ALMENDRAL J. A., SEOANE J. M. and SANJUÁN M. A. F., *Recent Res. Dev. Sound Vib.*, **2** (2004) 115.
- [22] NUSSE H. E. and YORKE J. A., *Dynamics: Numerical Explorations* (Springer, New York) 1997.